Transactions, SMiRT-26
Berlin/Potsdam, Germany, July 10-15, 2022
Division II

VERY HIGH CYCLE FATIGUE (VHCF) BEHAVIOR OF AUSTENITC STAINLESS STEELS AND THEIR WELDS FOR REACTOR INTERNALS AT AMBIENT AND OPERATING RELEVANT TEMPERATURE

Marek Smaga[1], Tobias Daniel[1], Elen Regitz[1], Tilmann Beck[1], Tim Schopf[2], Georg Veile[2], Stefan Weihe[2], Jürgen Rudolph[3], Udo Fischer[3]

[1] Institute of Materials Science and Engineering (WKK), TU Kaiserslautern, Germany (smaga@mv.uni-kl.de)
[2] Materials Testing Institute (MPA), University of Stuttgart, Germany
[3] Framatome GmbH, Erlangen, Germany

ABSTRACT

The fatigue assessment of safety relevant components is of importance for ageing management with regard to safety and reliability of nuclear power plants. Austenitic stainless steels are often used for reactor internals due to their excellent mechanical and technological properties as well as their corrosion resistance. During operation reactor internals are subject to mechanical and thermo-mechanical loading which induce low cycle (LCF), high cycle (HCF) and even very high cycle (VHCF) fatigue. While the LCF behavior of austenitic steels is already well investigated the fatigue behavior in the VHCF regime has not been characterized in detail so far. Accordingly, the fatigue curves in the applicable international design codes have been extended from originally 10^6 to the range of highest load cycles up to 10^{11} load cycles by extrapolation. Nevertheless, the existing data base for load cycles above 10^7 is still highly insufficient. The aim of the cooperative project of the Institute of Materials Science and Engineering (WKK) at University of Kaiserslautern, Materials Testing Institute (MPA) Stuttgart and Framatome GmbH, Germany is to create a comprehensive database up to the highest load cycles $N = 2 \cdot 10^9$ for austenitic stainless steels at ambient and elevated temperature. Hence, an elastic-plastic material model was developed to convert the displacement-controlled fatigue tests performed on an ultrasonic fatigue testing system to a total strain amplitude, which can be integrated into existing design codes and used to assess critical components.

INTRODUCTION

Low cycle fatigue occurs, e.g. in piping materials during heating and cooling cycles in start-up and shutdown operations due thermal stratification (Nagehsa et al. (2009)). Some nuclear power plants components additionally undergo high frequency loadings in the very high cycle fatigue regime e.g. by thermal striping and flow induced vibrations and their interaction. Thermal stripping is caused by fluid steams with temperature differences and a high rate of circulation which lead to turbulent mixing as shown schematically in Fig. 1a (Couturier and Schwarz (2020)), (Frank et al. (2010)). The resulting highly transient temperature fluctuations lead to cyclic thermal loading and consequently can results in the materials fatigue. As a consequence, surface cracks or so called elephant skin fracture and isolated cracks at weld beads were observed (Couturier and Schwarz (2020)). Therefore, the assessment of the VHCF behaviour, the treatment of fatigue damage accumulations in combination with the transient endurance limit and environmentally assisted fatigue are of high importance in the long-term operation context of reactor

internals but have not yet sufficiently been researched (Chopra and Shack (2007)), (Nuclear Safety Standards Commission (KTA) (2017))

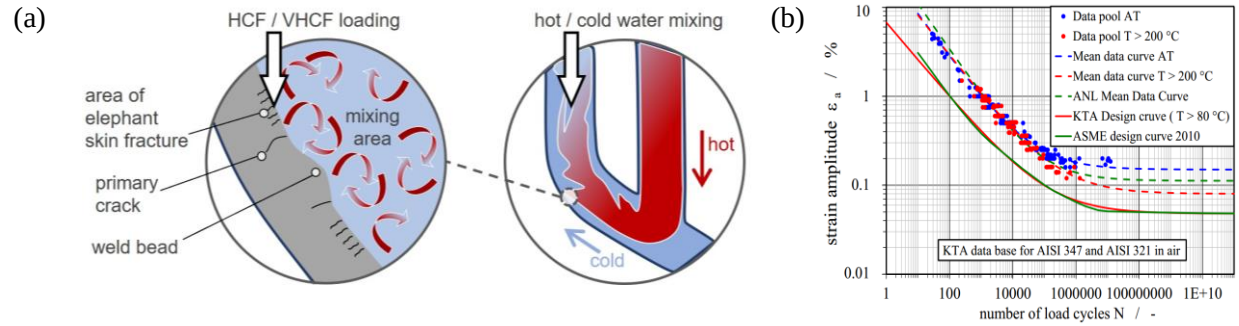

Figure 1. Schematic illustration of the simulation of the flow induced vibrations in a T-junction according to (Frank et al. (2010)) (a), KTA design curve (Schuler et al. (2013)) for the austenitic stainless steels AISI 347 and AISI 321 at ambient and operationally relevant temperature (b)

In Germany the joint research project titled “Investigation of the fatigue behaviour of austenitic stainless steels and their welds for reactor internals under high cycle and very high cycle operational loading conditions” supported by the Federal Ministry for Economic Affairs and Energy has the aim to close the mentioned gaps. Therefore, a data and assessment basis for the fatigue behaviour of unwelded and welded austenitic stainless steel components up to the highest load cycles $N = 2 \cdot 10^9$ at ambient temperature (AT) and at 300 °C were generated (Daniel et al. (2020)). For this purpose, a control rod guide tube was considered as an example for a relevant reactor structure with welded joints, since it is subjected to both, low cycle operational stresses from thermal stratification as well as flow forces and flow induced vibrations in very high cycle fatigue regime (Schuler et al. (2013)).

MATERIALS AND COMPONENTS

To investigate the fatigue behaviour of austenitic stainless steels and their welded joints for components in nuclear power plants, here on the example of a control rod guide tube, the austenitic base material AISI 347 / 1.4550 and the associated welded material ER 347 /1.4551 were used (Fig. 2).

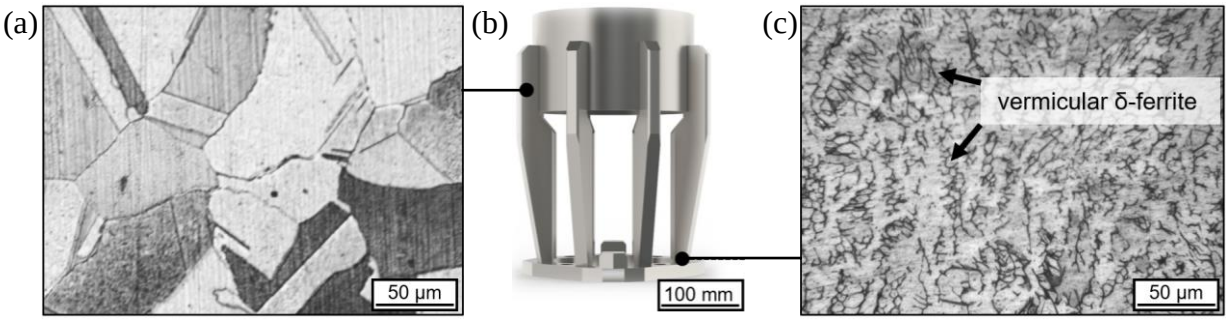

Figure 2. Microstructure of the base material, austentic stainless steel AISI 347 (a), CAD draw of a control rod guide tube (b) and microstructure of the the welded material ER 347 (c)

The specimens of the base material were extracted from an original nuclear power plant surge line pipe, which was not previously used for applications in nuclear power plants (Smaga et al. (2017)). The pipe was manufactured seamless and delivered in a solution annealed state (1050 °C / 10 minutes), such that in the

initial state purely austenitic microstructure was detected (Fig. 2a). At AT the AISI 347 indicates a metastable state so a deformation induced phase transformation from γ-austenite to α'-martensite can occur. Thereby, the stability of the austenitic phase increases with increasing temperature (Llewellyn (1997)). In order to investigate the welded material, an overmatched austenitic welded joint was produced consisting of several layers in accordance with KTA (German Nuclear Safety Standards Commission) standard. The specimens were extracted in the direction of the weld joint so the complete specimen consists of weld material. The weld material was heat threated at 580 °C for 100 minutes and shows δ-ferrite in a dendritic form (Fig. 2c). The pre-treatment of the materials as well as the microstructure and the quasi-static material behaviour are discussed in detail in (Daniel et al. (2020)). The chemical composition of the investigated materials is within the specifications of international standards as well as the KTA standards (Table 1) (German Institute for Standardization (DIN) (2014)), (Nuclear Safety Standards Commission (KTA) (2017)).

Table 1. Chemical composition of the investigated materials in wt.%

	Cr	**Ni**	**Mn**	**Nb**	**C**	**N**
AISI 347	14.6	10.64	1.83	0.62	0.04	0.007
ER 347	19.68	9.48	0.64	0.29	0.064	0.073

EXPERIMENTAL SETUP

To investigate the fatigue behaviour in the VHCF regime, high loading frequencies are essential to realize acceptable testing times (Stanzl-Tschegg (2014)). Hence, an ultrasonic fatigue testing (USFT) system was used to perform fatigue tests. Figure 3a shows the operating principle of the USFT which is based on the transformation of an ultrasonic electrical signal with 20 kHz into a mechanical oscillation with the same frequency.

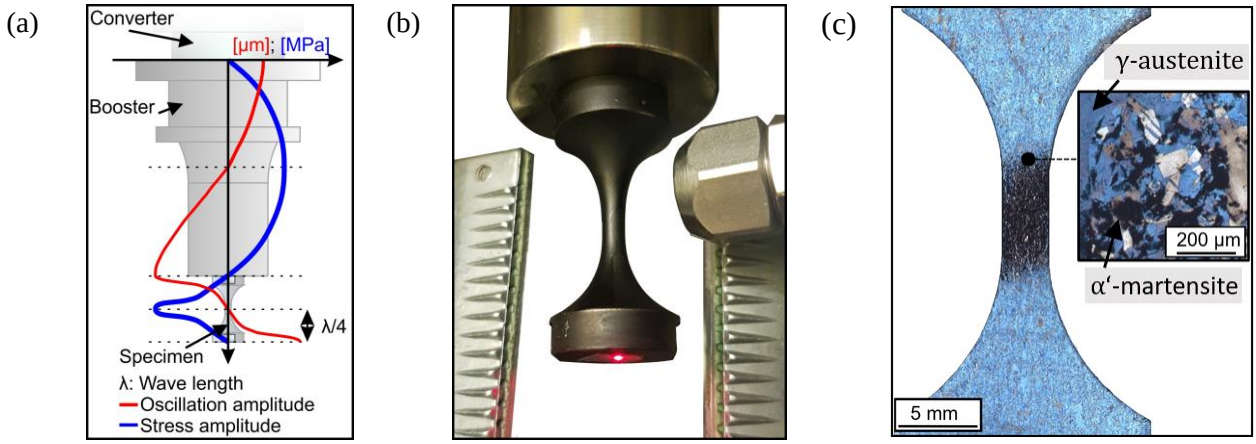

Figure 3. Operating principle of the ultrasonic fatigue (a), experimental setup at ambient temperature (b), microstructure in the longitudinal section at the transition of the specimen shaft to the gauge length of the metastable austenitic stainless steel AISI 347 after a load increase test at ambient temperature with ξ = 5.1 FE-% visualized by etching with Beraha I (c)

To ensure fully reversed loading conditions with the maximum displacement at the specimen end and the maximum stress in the centre of the gauge length, the specimens were designed for axial oscillation in the first Eigenmode at the operating frequency via dynamic FEM-simulation in ABAQUS software (2000).

Young's Modulus and Poisson's ratio determined in tensile tests were used as input data for the simulation leading to different geometries of the specimens for the two investigated materials at AT and 300 °C. The exact specimen geometries are shown in (Daniel et al. (2020)). An ultrasonic booster horn amplifies the mechanical oscillation in order to obtain the required stress/strain amplitudes in the specimen gauge section. The maximum stress amplitude was calculated via the linear relationship to the maximum displacement amplitude at the lower end of the specimen measured by a one-axis laser vibrometer. The calculation of the stress based on a linear elastic steady state analysis in ABAQUS (2000). Using an one-axis laser vibrometer to measure and control the displacement amplitude offers also the possibility to determine the exact number of cycles during high frequency loading (Daniel et al. (2022)). Due to a correct specimen design, the fatigue induced formation of α'-martensite occurred only in the gauge length of the specimen from metastable austenitic stainless steel AISI 347 (Fig. 3c). Similarly, crack initiation and specimen failure were observed in all fractured specimens exactly in the middle of the specimen. As a result of the self-heating of the investigated materials by high frequency cyclic loading, the tests were carried out in pulse-pause mode (Boemke et al. (2018)), (Smaga et al. (2019)), (Stanzl-Tschegg (2014)). In AT tests, the pulse-pause ratio was chosen in order to limit the absolute surface temperature of the specimen to 50 °C measured by a pyrometer. This resulted for the AISI 347 in effective frequencies of up to 1650 Hz at ambient temperature and up to 1800 Hz at 300 °C. For the isothermal fatigue tests at 300 °C, an induction heating system was integrated into the USFT system (Cavalieri et al. (2008)), (Daniel et al. (2020)). During these tests the set temperature deviation was less as 3 %. Due to a more stable material behaviour and the resulting lower self-heating, effective frequencies of up to 4000 / 2000 Hz could be achieved with the ER 347 at ambient respectively elevated temperature. More detail about VHCF fatigue tests on austenitic materials using USTF system is given in (Daniel et al. (2022)).

RESULTS

To characterize the cyclic deformation behaviour of the investigated materials, the dissipated energy which is defined as the integral of the ultrasonic generator power over the pulse time was used as a measured parameter. Accordingly, the dissipated energy is strongly dependent on the pulse time. An increase in dissipated energy, meaning the need of higher energy input for the oscillation and maintenance of the oscillation of the specimen for the same displacement amplitude, correlates with cyclic softening. In contrast, cyclic hardening is accompanied by a decrease in dissipated energy (Daniel et al. (2022)).

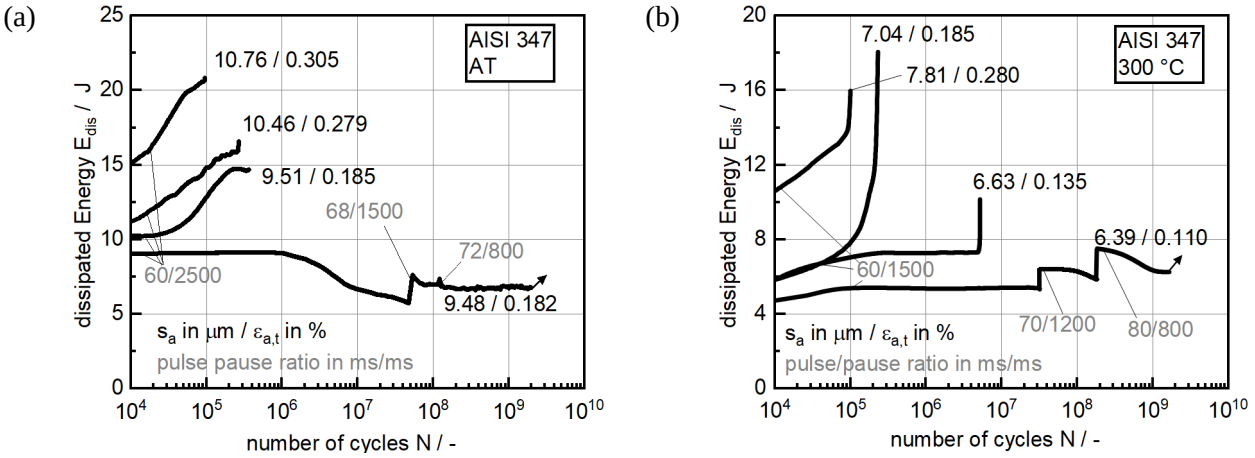

Figure 4. Cyclic deformation behaviour of AISI 347 characterized by change in the dissipated energy E_{dis} vs load cycles during testing using USFT system f = 20 kHz, R = -1, ambient temperature (a), 300 °C (b)

Figure 4 shows for selected tests that the metastable austenitic stainless steel AISI 347 exhibited consistent cyclic softening at both temperatures (AT and 300 °C) for higher displacements, resulting in specimen failure below 10^7 load cycles. Crack initiation took place on the specimen surface at slip bands. Lower displacements led to stable material behaviour at ambient temperature up to approx. 10^6 load cycles and subsequent hardening until the limiting load cycle number was reached. The hardening, which was accompanied by a lower self-heating, enabled the increase of the pulse time, which resulted in abrupt jumps in the course. For better understanding, the used pulse pause times are indicated in the diagram. This material behaviour correlated with the phase transformation from γ-austenite to α'-martensite in the AISI 347 and led to phase contents up to 2.4 FE-%. FE-% is measured unit of magnetic inductive feritscope™ sensor and correlated directly with the amount of ferromagnetic α´-martensite (Talonen et al. (2004)). At 300 °C, cyclic softening occurred first at lower displacements, followed by a saturation state and subsequent hardening, which also resulted in reaching the limiting load cycle number. Despite increased austenite stability at 300 °C, small amounts of martensite of up to 0.9 FE-% were formed only in run-out specimens. Analogously, the cyclic deformation behaviour of the weld material ER 347 is shown in Figure 5. Cyclic softening as a result of high displacements also resulted in specimen failures below 10^7 load cycles for both temperature levels. Crack initiation occurred at pores on the surface resulting from the welding process. At lower stresses, stable material behaviour was observed without hardening or softening processes that finally led to achieving the limiting number of cycles. Compared to AISI 347, the ER 347 did not show any α'-martensite formation during the fatigue tests.

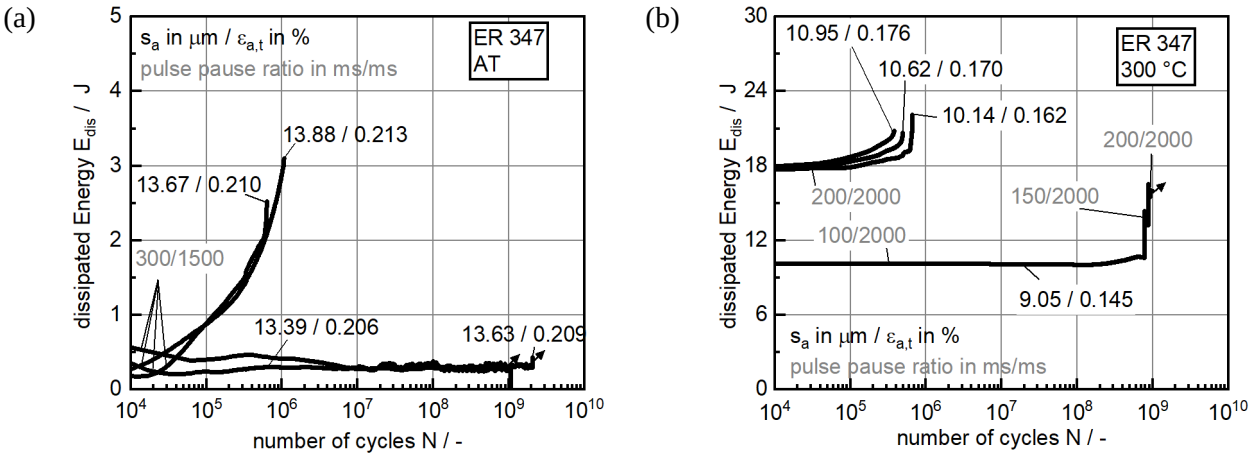

Figure 5. Cyclic deformation behaviour of ER 347 characterized by change in the dissipated energy E_{dis} vs load cycles during testing using USFT system f = 20 kHz, R = -1, ambient temperature (a), 300 °C (b)

The lifetime-oriented analysis of the VHCF tests is shown in Fig. 6 in the form of Woehler diagrams. As can be seen there is no material failure in the VHCF regime for both materials. While in the case of AISI 347 the hardening material behaviour leads to the formation of a true fatigue strength, in the case of ER 347 the extended lifetime of the material can be explained by the fact that below a certain stress level no more damage occurs. Furthermore, it is evident that for the investigated materials the fatigue strength decreases with increasing temperature. As mentioned, the displacement-controlled VHCF tests were converted usually linearly elastically and transformed directly into stress or strain fatigue life curves. However, the cyclic deformation behaviour especially of AISI 347 suggests an elastic-plastic material behaviour due to the pronounced softening and hardening processes, even by a small total-strain amplitude of $\varepsilon_{a,t}$ = 0.10 % from VHCF regime (see Fig. 7). Consequently, the linear elastic consideration can't be correct. To predict the lifetime of components an exact reproduction of the material behaviour is required to achieve realistic results with numerical simulations. Stress-strain curves for a specimen in relation to the time must be estimated precisely to avoid inaccuracies. Figure 7a depicts the cyclic deformation for fatigue tests at

ambient temperature emphasizing the cyclic hardening effect for the AISI 347. Figure 7b shows the cyclic deformation behaviour at 300 °C (Schopf et al. (2021)).

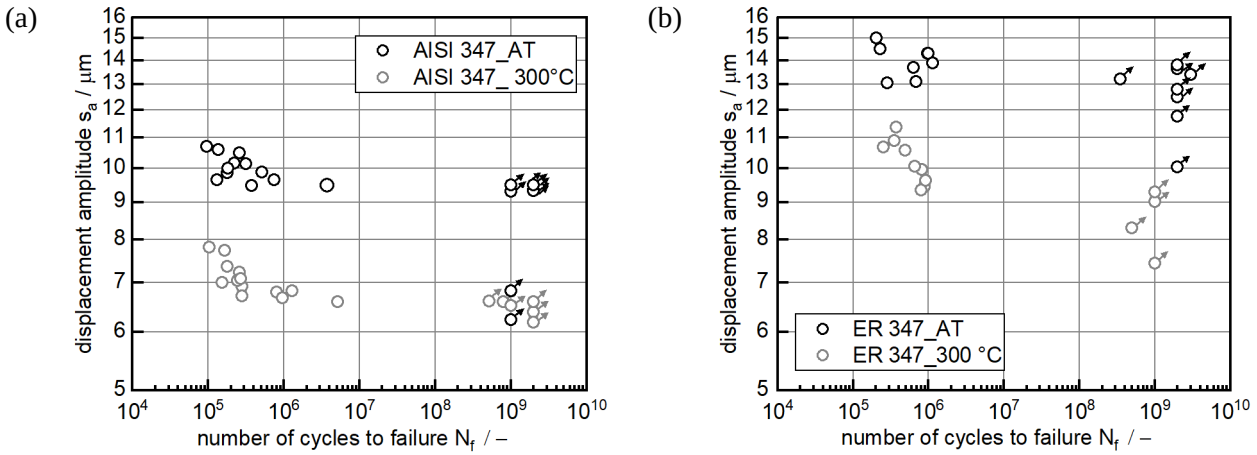

Figure 6. Fatigue life data; displacement amplitude versus number of cycles to failure at ambient temperature and 300 °C for AISI 347 (a) and ER 347 (b)

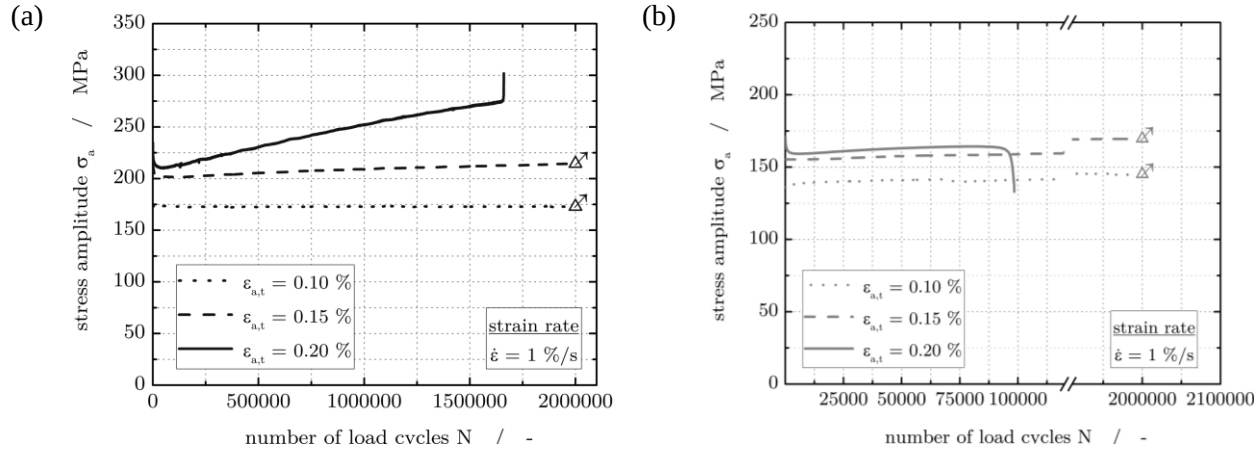

Figure 7. Cyclic deformation curves for fatigue tests with the load amplitude form HCF regime ($\varepsilon_{a,t}$ = 0.20 %), from the HCF-VHCF transition ($\varepsilon_{a,t}$ = 0.15 %) and from the VHCF regime ($\varepsilon_{a,t}$ = 0.10 %) at ambient temperature (a), at 300 °C (b)

The lack of material model parameters of metastable austenitic stainless steel AISI347 for the VHCF regime led to the requirement of experiments to obtain stress-strain-hysteresis from cyclic deformation curves (Daniel et al. (2020)). The determined stress-strain-hysteresis at ambient temperature and 300 °C are illustrated in Figure 8. The representative illustration shows a significant elastic-plastic material behaviour up to the VHCF regime ($\varepsilon_{a,t}$ = 0.10 %) and supports the need for a realistic material model. To take these material effects into account, a basis model of the elastic-plastic material model was developed for the two materials to evaluate the ultrasonic-based fatigue tests in the VHCF regime. This model, based on Armstrong-Frederik and Chaboche (AFC) with kinematic laws, was used and described in detail by (Daniel et al. (2020)), (Schopf et al. (2021)). Required parameters of AFC derived from experimental data and an optimization algorithm to determine an accurate stress-strain behaviour. Since total-strain controlled LCF and displacement controlled VHCF tests differ in their control mode, each test requires its own evaluation.

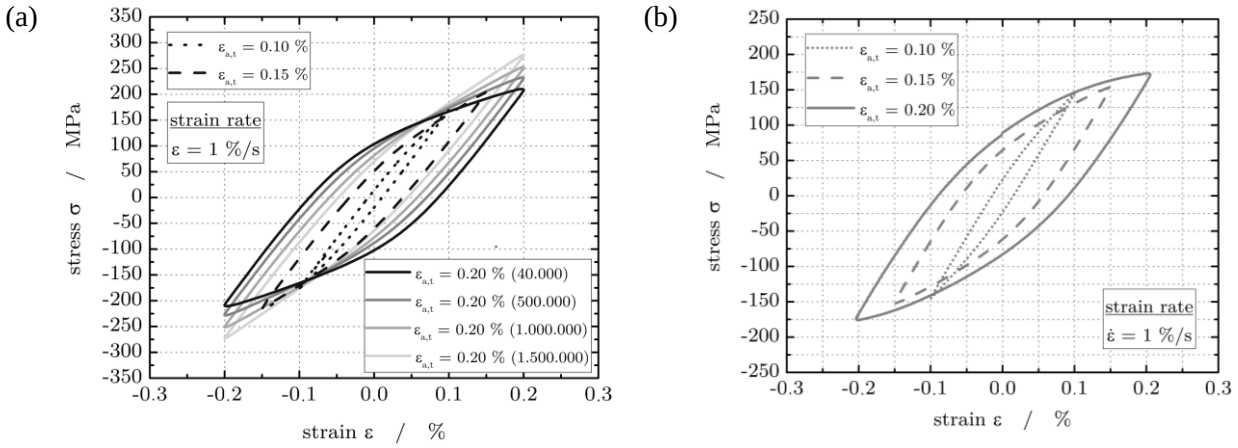

Figure 8. Representative stress-strain-hysteresis for load levels in the HCF regime ($\varepsilon_{a,t}$ = 0.20 %), the HCF/VHCF transition ($\varepsilon_{a,t}$ = 0.15 %) and in the VHCF regime ($\varepsilon_{a,t}$ = 0.10 %) at ambient temperature (a), 300 °C (b)

In ultrasonic fatigue tests stress distribution in the specimen differs fundamentally compared to conventional fatigue tests. Furthermore, occurring stresses by ultrasonic testing are determined by vibration analysis as explained in the previous section. Purely dependent elastic material properties are combined with an elastic-plastic material model. At this point it should be noted that the α'-martensite formation occurring in experiments is also considered since this leads to cyclic hardening of the material. By combining a numerical model of the steady state dynamic analysis with cyclic stress-strain curves the elastic-plastic strain amplitude can be determined. The results for the AISI 347 shown in Fig. 9 have been calculated using the evaluation concepts described before. In both result diagrams, ambient temperature (a) and 300 °C (b), the fictitious-elastic evaluations are additionally shown as a basis for comparison.

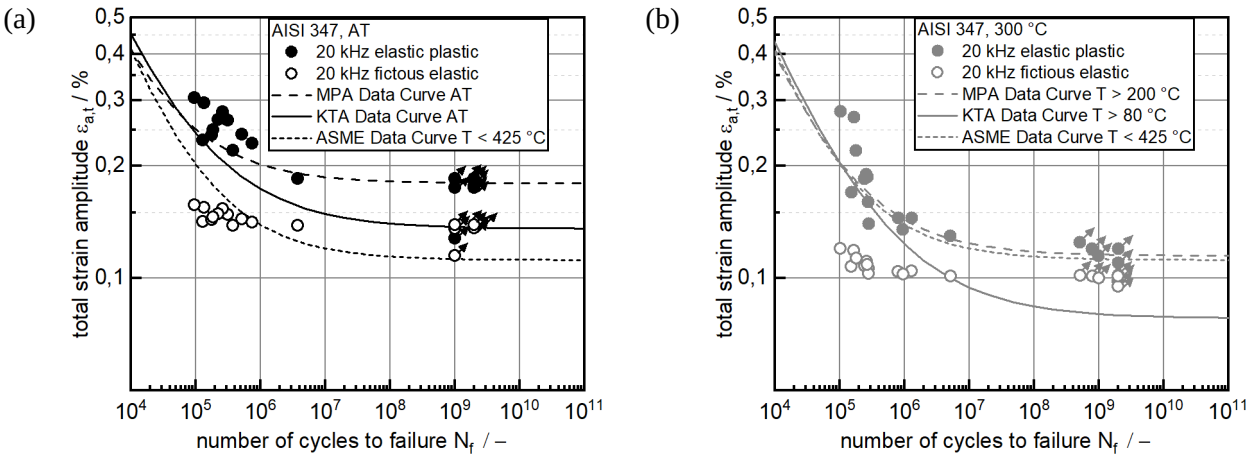

Figure 9. Calculation of a total strain amplitude fatigue life curve with a fictitious elastic assessment method and with the elastic-plastic VHCF material model for AISI 347 at ambient temperature (a), 300 °C (b)

As can be seen in Fig. 9, the experimental results in the VHCF regime for the AISI 347 assessed with a fictitious elastic method are not valid because the material shows cyclic plasticity in the VHCF regime. For

this reason, the data points are far on the conservative side in terms of both fatigue life and fatigue strength. At ambient temperature the KTA and ASME (American Society of Mechanical Engineers) mean data curves are way too conservative. New proposals are made by MPA (Schopf et al. (2021)) mean data curves to cover the data in the HCF/VHCF regime and the endurance limit. For 300 °C a comparison with the mean data curve given by the ASME code shows that the elastic-plastic evaluation methods lead to a good agreement. The previous assumptions and curves based on extrapolation in the VHCF regime could thus be validated experimentally. This not only describes the relationship between stress level and service life in the HCF/VHCF regime, but also makes it possible to quantitatively determine a fatigue limit for ambient temperature and at an operationally relevant temperature of 300 °C. Similarly, the results for the weld material ER 347 are shown in Fig. 10 for both ambient temperature and 300 °C. Due to the significantly lower cyclic plasticity in the VHCF regime, there is almost no difference between the linear elastic and the elastic-plastic evaluation methods, especially at ambient temperature. Comparison of the results for both temperature levels with the corresponding mean data curves shows that they underestimate the fatigue strength of the material in the VHCF regime. As with the results on AISI 347, the results on ER 347 also allow a quantitative assessment of the fatigue limit for ambient temperature and 300 °C.

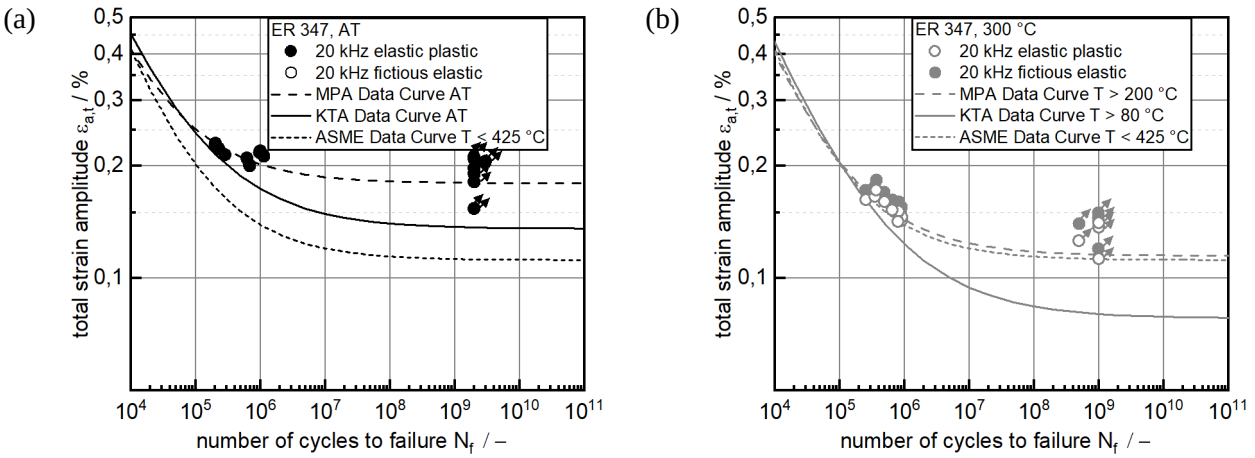

Figure 10. Calculation of a total strain amplitude fatigue life curve with a fictitious elastic assessment method and with elastic-plastic VHCF material model for ER 347 at ambient temperature (a), 300 °C (b)

Based on the experimental fatigue tests, the fatigue assessment example of a control rod guide tube is done by a setup of two finite element models with the FEM ANalysis SYStem (ANSYS) software. Two models were developed (i) for LCF loading and (ii) VHCF loading. Both Figures, 11a and 11b show the VHCF loading configuration of fluid dynamical induced vibrations during the reactor operation. Both models contribute to the overall fatigue usage, but the second model for VHCF assessment is discussed in more detail here. The first investigation comprised the recalculation of a former fatigue assessment to reproduce the relevant section loads acting in the control rod guide tube welding connections. The mechanical loads acting on the VHCF model are fluid dynamical induced vibrations during the reactor operation. The control rod guide tube elongation is caused by the shape of the natural frequency and is chosen as the relevant structural load. After a modal analysis the displacement vector of the natural frequency mode is applied in a scaled manner onto the model. This vectorial scaling is adjusted taking into account the available space for the control rod guide tube deflection in the installation area, to be representative for the possible maximum deflection of the control rod guide tube model. The objective of recalculation of the former FEM investigation is fulfilled in regard to the natural frequency, deformation shape, general stress level, location of stress maximum and height of intersection loads. Therefore, the current ANSYS model is appropriate for further VHCF fatigue assessments. The next project step is to select a sub model region of a welded

area, and to apply the local intersection loads with the help of a peak stress fatigue modelling scenario. The material characteristics curves and parameters shall be chosen from the material test results developed during this project. The fatigue assessment methods developed as part of the project including a damage parameter approach are going to be applied to this example. This requires a detailed model of the weld seem including the weld toes.

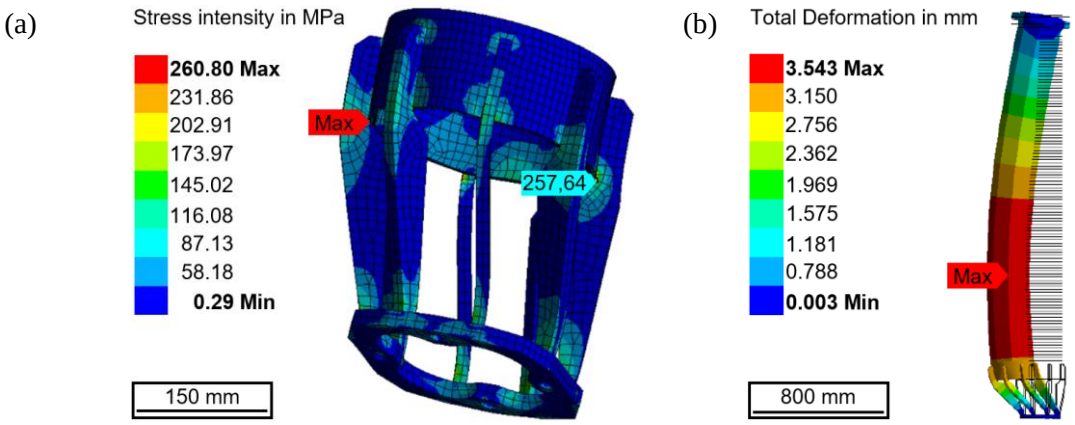

Figure 11. Fatigue assessment of a control rod guide tube: stress level of the natural frequency with a scaled deflection of 1 mm (a), shape of the natural frequency with the calculated maximum deflection (b)

CONCLUSION

The results of the research project on the fatigue behaviour of the metastable austenitic steel AISI 347 and the welded material ER 347 show that for both materials there is no fatigue failure in the VHCF regime both at ambient temperature and at 300 °C and that a true fatigue strength exists above 10^7 load cycles. The analysis of the cyclic deformation behaviour shows that in the case of AISI 347 cyclic hardening leads to the formation of a true fatigue strength. The welded material ER 347 shows a stable cyclic deformation behaviour and also true fatigue endurance limit. Taking into consideration the elastic-plastic behaviour of metastable austenitic stainless steels AISI 347 in the VHCF regime, a material model was developed, which allows a comprehensive recalculation of the displacement-controlled fatigue tests in the total strain-controlled fatigue tests amplitude. Thus, can be included in the design curves of the codes. Furthermore, simulations of critical components under both high-frequency and thermal cycling loads were performed and evaluated for reliability using the results of the fatigue tests.

ACKNOWLEDGEMENTS

The authors thank the Federal Ministry for Economic Affairs and Energy (BMWi), Germany for the financial support. Reactor Safety Research, project numbers 1501548 and 1501636.

REFERENCES

Boemke, A., Smaga, M. and Beck, T. (2018). *Influence of surface morphology on the very high cycle fatigue behavior of metastable and stable austenitic Cr-Ni steels*. MATEC Web Conf. 165.

Cavalieri, F., Bathias, C., Ranc, N., Cardona, A. and Risso, J. (2008). *Ultrasonic fatigue analysis on an austenitic steel at high temperature*. Mecánica Computacional 27:1205–24.

Chopra, O. K and Shack, W. J (2007). *Effect of LWR Coolant Environments on the Fatigue Life of Reactor Materials*. Final Report, NUREG/CR-6909 47527.

Couturier, J. and Schwarz, M. (2020). *Current state of research on pressurized water reactor safety*.

Daniel, T., Smaga, M. and Beck, T. (2022). *Cyclic deformation behavior of metastable austenitic stainless steel AISI 347 in the VHCF regime at ambient temperature and 300 °C*. Int. J. Fatigue 156:106632.

Daniel, T., Smaga, M., Beck, T., Schopf, T., Stumpfrock, L. and Weihe, S. et al. (2020). *Investigation of the very high cycle fatigue (VHCF) behavior of austenitic stainless steels and their welds for reactor internals at ambient temperature and 300 °C*. Proc. ASME PVP Conf. 83815.

Frank, T., Lifante, C., Prasser, H.-M. and Menter, F. (2010). *Simulation of turbulent and thermal mixing in T-junctions using URANS and scale-resolving turbulence models in ANSYS CFX*. Nuclear Engineering and Design 240 (9):2313–28.

German Institute for Standardization (2014). *DIN EN 10088-1*: Stainless steels - Part 1: List of stainless steels; German version EN 10088-1:2014.

Llewellyn, D. T (1997). *Work hardening effects in austenitic stainless steels*. Mater Sci Technol 13 (5).

Nagehsa, A., Valsan, M., Kannan, R., Bhanusankararao, K., Bauer, V. and Christ, H. et al. (2009). *Thermomechanical fatigue evaluation and life prediction of 316L(N) stainless steel*. International Journal of Fatigue 31 (4):636–43.

Nuclear Safety Standards Commission (2017). *KTA 3201.1 Components of the Reactor Coolant Pressure Boundary of Light Water Reactors; Part 1: Materials and Product Forms*.

Nuclear Safety Standards Commission (2017). *KTA 3204: Reactor Pressure Vessel Internals*.

Schopf T, Stumpfrock L, Weihe S, Daniel T, Smaga M, Beck T et al. *Untersuchungen zum Ermüdungsverhalten austenitischer Werkstoffe und deren Schweißverbindungen für RDB- und Kerneinbauten im HCF- und VHCF-Bereich (VHCF-I)*: BMWi - 1501548. final report (2021.

Schopf, T., Weihe, S., Daniel, T., Smaga, M., Beck, T. and Rudolph, J. (2021). *Fatigue Behavior and Lifetime Assessment of the Austenitic Stainless Steel AISI 347 and its Associated Filler Metal ER 347 Under Low-, High- and Very High Cycle Fatigue Loadings*. Proc. ASME PVP Conf.

Schuler, X., Herter, K.-H. and Rudolph, J. (2013). *Derivation of Design Fatigue Curves for Austenitic Stainless Steel Grades 1.4541 and 1.4550 Within the German Nuclear Safety Standard KTA 3201.2*. Proc. ASME PVP Conf.

Smaga, M., Boemke, A., Daniel, T., Skorupski, R., Sorich, A. and Beck, T. (2019). *Fatigue Behavior of Metastable Austenitic Stainless Steels in LCF, HCF and VHCF Regimes at Ambient and Elevated Temperatures*. Metals 9.

Smaga, M., Sorich, A., Eifler, D. and Beck, T. (2017). *Very high cycle fatigue behavior of metastable austenitic steel X6CrNiNb1810 at 300°C*. Proc. 7th Int. Conf. on VHCF:249–54.

Stanzl-Tschegg, S. E (2014). *Very high cycle fatigue measuring techniques*. Int. J. Fatigue 60:2–17.

Talonen, J., Aspegren, P. and Hänninen, H. (2004). *Comparison of different methods for measuring strain induced α-martensite content in austenitic steels*. Mater Sci Technol 12:1506–12.

Ultrasonic Fatigue Testing (2000). In: ASM Handbook, 8th ed., p. 1650–1681.